Norwegian Meteorological Institute
met.no

met.no report

Report no. 21/2010
Oceanography
ISSN: 1503-8025
Oslo, December 22, 2010

LOVECUR Final Report: Description of model and discussion of the model results

Lars Petter Røed and Nils Melsom Kristensen

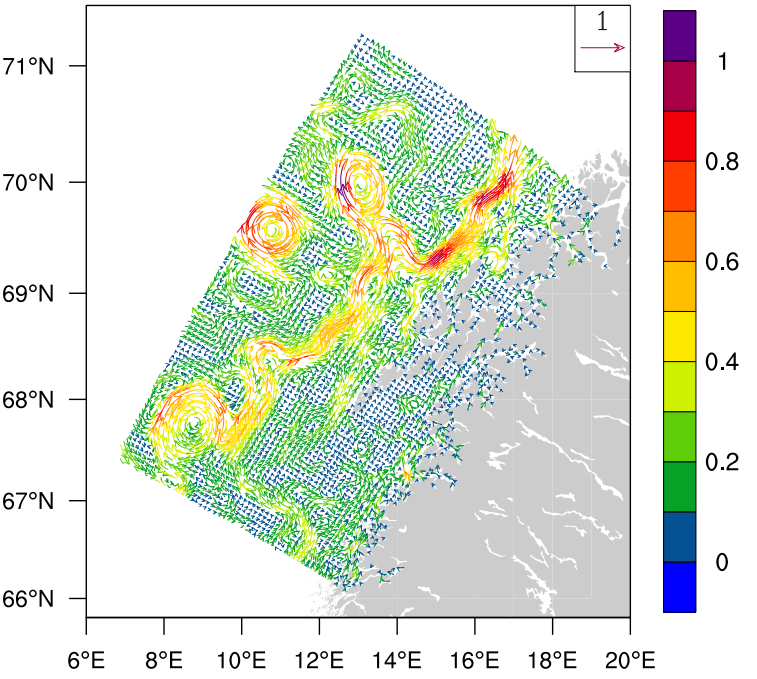

INSTITUTE OF MARINE RESEARCH
HAVFORSKNINGSINSTITUTTET

Norwegian Meteorological Institute
met.no

Norwegian Meteorological Institute
met.no

report

Number	Subject	Date	Classification	ISSN
21/2010	Oceanography	December 22, 2010	☒ Open ☐ Restricted ☐ Confidential	1503-8025

Title

LOVECUR Final Report: Description of model and discussion of the model results

Authors

Lars Petter Røed and Nils Melsom Kristensen

Client(s)	Client reference
Statoil (Børge Kvingedal)	Contract No. 452047180

Abstract

We have performed a one and half year simulation of currents in the Lofoten-Vesterålen area covering a period from January 2, 2009 to June 30, 2010. For this purpose we have used the numerical ocean model ROMS. Its atmospheric input is derived from archived 12 km HIRLAM analyzes. At the open lateral boundaries we use archived daily mean fields from the MIPOM analyzes. As tidal forcing we use the TPXO data base. The first half year is a spin up and data are only stored for the period July 1, 2009 through June 30, 2010. Required model results at nine predefined locations are extracted together with results from a host of other locations corresponding to locations where Institute of Marine Research (IMR) have made measurements in the Lofoten-Vesterålen area. The required model results consists of current speed and direction at 10 m depth intervals, temperature and salinity at 10 m depth intervals and tidal height and storm surge. Finally we show some model-data comparison using the IMR data. The comparisons are done in terms of time series and frequency diagrams (PDFs). The model results show that the model is definitely eddy resolving giving a zoo of eddies due to the existence of the unstable front separating Norwegian coastal water from warmer water of Atlantic origin along the shelf slope. We conclude that although the model is far from being perfect it gives a reasonable realistic picture of current and hydrographic conditions in the study area.

Keywords

Physical Oceanography, Numerical Modeling, Mesoscale

Disiplinary signature	Responsible signature
Øyvind Sætra, Head Section Oceanography	Øystein Hov, Head Research and Development Department

Postal address
PO Box 43 Blindern
N-0313 Oslo
Norway

Office
Niels Henrik Abels vei 40

Telephone
+47 2296 3000

Telefax
+47 2296 3050

e-mail: met.inst@met.no
Web: met.no

Bank account
7695 05 00601

Swift code
DNBANOKK

Executive summary

We consider the results from a one year simulation employing the numerical ocean model ROMS on an eddy resolving grid (mesh size of $\sim$ 820 m) for a region along the Northern coast of Norway, specifically the Lofoten-Vesterålen (LV) area (Figure 1). ROMS employs a generalized terrain-following coordinate which allows high vertical resolution near the surface even in the deep water areas off Lofoten.

The particular aim of the study is to assess whether the simulated numerical ocean weather is able to reproduce what is observed. Ocean weather is connected to eddies, jets and meanders with a typical length scale of order 10 km in these waters. It should be emphasized that these features are responsible for most of the high current events in the ocean. The present results are to be compared with other numerical ocean weather simulations by a third party.

Since we at present do not have access to any current observations for the hindcast/simulation period (July 1, 2009 through June 30, 2010) we focus on a comparison with temperature and salinity data extracted from the Institute of Marine Research's hydrographic data base. In light of the active, small scale eddy field giving rise to a high spatial and temporal variability in the area (e.g., Figure 11) we focus on *statistical* comparisons of time series. In addition we have examined the spatial structure (lateral and vertical) of the velocity means (yearly, monthly and daily means) at different depths.

The simulated one year mean flow (Figure 8) is generally in line with a similar product constructed from observations alone (Figure 7). A primary difference is that the ROMS mean along-slope jet is narrower and more energetic than the jet estimated from observations, with generally higher speeds in the ROMS means. The flow pattern is however very similar with an intensification of the northward flowing jet west of Lofoten. The jet is clearly baroclinically unstable (*Shi and Røed*, 1999; *Fossum and Røed*, 2006) shedding off eddies of diameter $\sim$ 40-50 km, and a host of smaller scale eddies (Figure 11). The larger scale eddy is a long-lived feature once formed and hence shows up in the monthly mean fields as well (Figure 9).

A comparison of the observed temperature and salinity with those of ROMSreveals that the model has a fresh bias of about 0.3 psu. Also revealed is that model tends to be too cold in the summer and too warm in the winter.

Contents

List of Tables

List of Figures

List of abbrevations used

Here is a list of the main abbreviation used in the text.

- HIRLAM = High Resolution Limited Area Model
- LV = Lofoten-Vesterålen
- LOVECUR = The version of the model ROMS set up for the Lofoten-Vesterålen area
- IMR = Insitute of Marine Research, Bergen, Norway
- met.no = The Norwegian Meteorological Institute, Oslo, Norway
- MIPOM = Norwegian Meteorological Institute's version of the Princeton Ocean Model
- NIVA = Norwegian Institute of Water Research, Oslo, Norway
- NorKyst800 = A collaborative project by and between met.no, IMR and NIVA to establish a fine mesh ocean predictive model for Norwegian coastal waters. The target mesh size is 800 m (*Albretsen et al.*, 2010)
- NCC = Norwegian Coastal Current flowing along the Norwegian coast from the Swedish border to the Barents Sea.
- NCW = Norwegian Coastal Water. NCW is commonly defined as water of salinity less than 34.5 psu (*Sætre*, 2007c).
- PDF = Probability density distributions, sometimes also referred to as frequency diagrams
- POM = Princeton Ocean Model
- ROMS = Regional Ocean Modeling System
- www.yr.no = The Norwegian Meteorological Institute web portal for dissemination of atmospheric and ocean weather forecasts
- SSH = Sea surface height. Contains the combined water level due to tides and storm surges.

1 Introduction

The purpose of this report is to provide an overview of the work performed by the Norwegian Meteorological Institute (met.no) associated with research Contract No. 452047180 awarded to met.no by Statoil. The work is part of a Joint Industry Project to enhance our understanding of currents in the Lofoten and Vesterålen (LV) area (Figure 1). To prepare for eventual oil and gas exploration it is of general importance to get a good understanding of the environment in the LV area. In particular it is of interest to get insight into the meteorological and oceanographic variables such as winds, waves, water level (tidal height and storm surge) and currents to design offshore structures that are both safe and cost efficient.

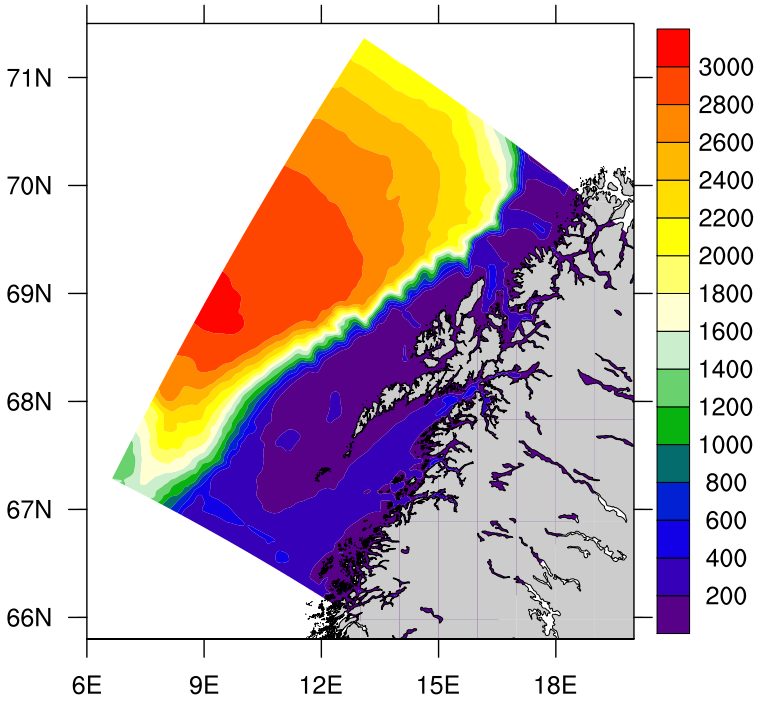

Figure 1: Displayed is the computational domain of the LOVECUR model and its rendition of the topography in the Lofoten-Vesterålen area. The color coding shows depths in meters in accord with the color bar on the right-hand side. Note the many small scale canyons and promontories along the shelf break.

The focus here is to provide increased understanding of the above ocean variables in the LV area. To this end the Norwegian Meteorological Institute is asked, as one of several institutions, to provide detailed information about currents, water level, temperature and salinity for the period from July 1, 2009 to July 1, 2010 in the LV area, by use of numerical ocean models, that is, to perform a hindcast simulation at least one year long. The information will a posteriori be used to evaluate the model's skill in hindcasting currents by a third party in comparison with other similar simulations performed by other institutions.

In general the currents in the LV area consist of the northward flowing current known as the Norwegian Coastal Current exhibiting maximum speeds of about 1 m/s. The main path of the current follows the shelf slope and is associated with the front that separates the inflowing high salinity water of Atlantic origin from the fresher coastal water. As in the atmosphere these fronts are unstable and on the shelf and off the shelf high current speed events are commonly associated with features such as mesoscale eddies, fronts and jets, or simply features associated with what may be referred to as the oceanic weather. The term 'oceanic weather' is used since the mesoscale eddies, jets and fronts are the oceanic counterpart to the atmospheric cyclones. In Norwegian ocean waters these features typically have a length scale of order 10 km which is two order of magnitude smaller than in the atmosphere. To be able to forecast such events is of importance for all kinds of operations at sea including operations performed by the offshore industry.

Just as in meteorology ocean forecasts are based on numerical models. The question therefore arises: what is the model's skill? For marine operations the focus is traditionally on the model's skill in forecasting a particular event, say an extreme current event. We may refer to this skill as the model's forecast skill. When designing offshore structures the focus is shifted to the model's skill in reproducing the statistics, in which case the skill we refer to is the model's statistical skill. The latter refers to the model's ability to reproduce known statistical properties for instance the frequency of extreme current events. It should be emphasized that even though the model's forecast skill is poor, the model's statistical skill may still be fairly good, but not vice versa. The reason for this is that the model may have a poor timing of the various extreme events, but the number of such events, say eddies passing a particular location during a season or year, may still be correctly simulated. Under these circumstances the forecast skill will be poor, but the model's statistical skill will be good. While a model's forecasts skill is reasonably well analyzed by simple scatter diagrams, the model's statistical skill is best assessed by analyzing the frequency distribution of events or so called probability density functions (PDFs). Thus to evaluate the skill of a particular model we must not only consider its ability to forecast particular events in the ocean, but also consider its ability to reproduce known statistical properties. The latter is for instance of importance in the design of offshore structures where the tail or wings of the distributions are of crucial importance to simulate correctly.

The work performed for this particular purpose builds on met.no's capability to produce current hindcasts and forecasts in Norwegian waters (*Martinsen et al.*, 1995; *Engedahl*, 1995b; *Engedahl and Røed*, 1999; *Hackett and Engedahl*, 2000; *Engedahl et al.*, 2001; *Jenkins et al.*, 2001; *Røed and Fossum*, 2004; *LaCasce and Engedahl*, 2005; *Fossum*, 2006; *Albretsen*, 2007; *Røed and Albretsen*, 2007; *Albretsen and Røed*, 2010). To this end met.no for many years used a local version of the ocean model POM (*Blumberg and Mellor*, 1987) named MIPOM (*Engedahl*, 1995b; *Engedahl et al.*, 2001). Presently MIPOM is replaced by a more modern and recently developed ocean model named ROMS. For the time being, they both run in parallel and are set up to produce up to 66 hours forecasts once a day year round for Norwegian waters. These forecast includes smaller local domains, with eddy resolving capacities, nested into a the main forecasting model. The latter covers the entire Nordic Seas with a grid size of 4 km. Daily updates of the latter forecasts are available at the web portal www.yr.no.

Recently met.no in collaboration with the Institute of Marine Research (IMR) and the Nor-

wegian Institute of Water Research (NIVA) embarked on a project with the goal of establishing a fine mesh ocean model for the Norwegian Shelf areas with a grid size of 800 m (hereafter NorKyst800). Moreover, as part of the MyOcean project (myocean.eu.org) funded by the European Commission's seventh Framework Programme, met.no in collaboration with the Nansen Environmental and Remote Sensing Center, is also responsible for running and disseminating operational forecast products from the TOPAZ system (available at the site myocean.met.no).

The present work take advantage of the work done in NorKyst800 in that we use the bottom topography and land sea mask already provided, and use this to cut out a nested model domain as displayed on the front page figure. In Sections 2 and 3 we describe this work in more detail and also provide information about the models we use. In Section 4 we describe and analyse the results and include a thorough discussion of the results. Since the models velocity distributions and the wings of these distributions are important for establishing the design currents, we focus in particular on how good the models are at capturing the higher end of the velocity distributions. A summary is provided in the Executive summary up front and also in Section 5.

2 Configuration of the model

In setting up the LOVECUR version of ROMS for the one year simulation covering the LV area there is some crucial input needed. This includes definition of the computational domain and the topography. Other important input is mesh size, atmospheric driving forces (momentum, freshwater and heat fluxes), input from rivers, tidal forcing, initial conditions and lateral forcing at open ocean boundaries.

2.1 Computational domain

The computational domain and area of the LOVECUR model is displayed in Figures 1 and 2. The major topographic feature of the LV area is the steep shelf slope in which the depth changes from about 200 m on the shelf to an abyss of about 3000 meters deep in the Lofoten basin. The lateral distance over which this happens is only 30 to 40 km. Furthermore we note that the shelf is highly irregular with small scale canyons and promontories cutting across it. The circulation in the upper water layers is dominated by an inflowing jet that follows the shelf slope northwards. The jet is associated with the front separating the coastal water masses, comprised of the fresh and (in winter) cold Norwegian Coastal Water (NCW), from the saltier and warmer inflowing water of Atlantic origin (*Sætre*, 2007a) as for instance depicted by Figures 3. The front is unstable and the LOVECUR area is therefore a region of complex dynamics, with many mesoscale features such as eddies, fronts and jets (*Sætre*, 2007b) which is also depicted by our model results (Figure 4). In particular we note the robust eddy located in the vicinity of 69°N, 12°E, an eddy also noted by *Røed et al.* (2010). As argued by *Fossum and Røed* (2006), *Fossum* (2006) and *Albretsen* (2007) these structures are dynamically similar to the cyclone systems found in the atmosphere, and are caused by a combination of baroclinic

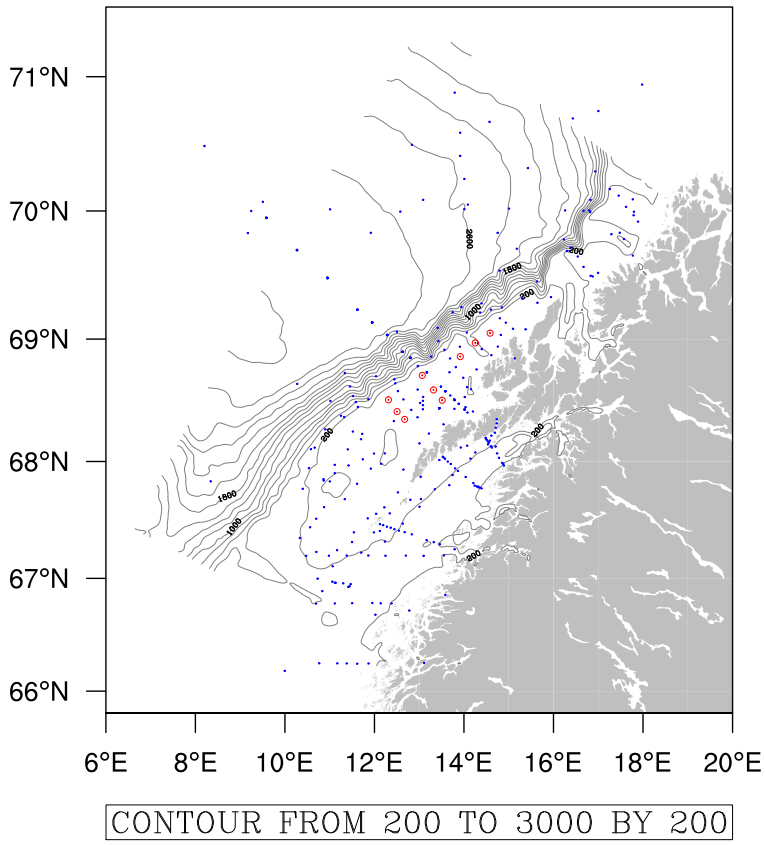

Figure 2: Displayed are bottom topography contours and location of IMR hydrographic stations (blue dots) used for validation purposes in the LV area or. Also shown (red dots) are the locations of the nine stations at which contracted time series of model results are extracted. Note that most of the hydrographic stations are on the shelf in water of depths less than 200 m, and that all of the stations were model results are extracted are on the shelf.

and barotropic instabilities. Moreover they are associated with strong velocities and, as is well known, constitute a potential threat to any offshore and/or marine operation.

2.2 Model set up

2.2.1 Mesh size

The mean mesh size is slightly about 820 m with a maximum mesh size of 835 m and a minimum mesh size of 815 m. Note that this relative fine mesh makes the models eddy resolving. We emphasize that the phrase eddy resolving is used to acknowledge that the model not only resolve the eddies once formed, but also the processes that cause mesoscale features in general and eddies in particular to be generated. The one and a half year simulation commenced on

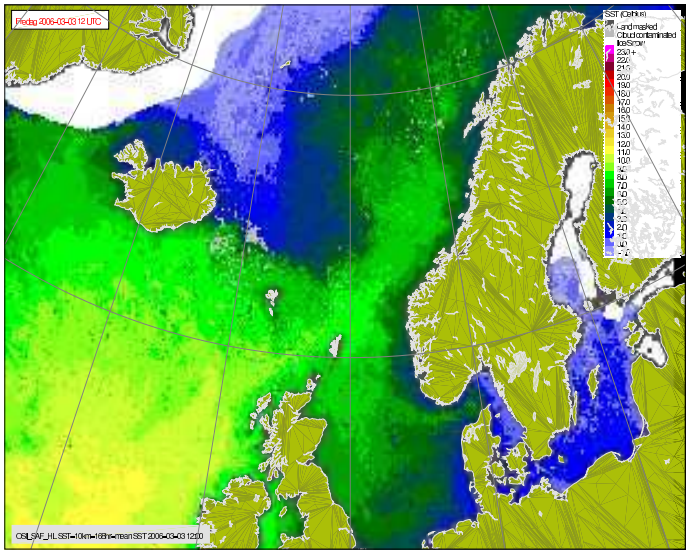

Figure 3: Satellite image depicting the sea surface temperature (SST) in the northern North Atlantic. The image is a one week composite centered on March 3, 2006, with a contour interval of 1°C. This and similar images are available at http://saf.met.no/.

January 2, 2009 00UTC and ended on June 30, 2010 00UTC. The first half year is a spin up and results are only shown for the last year.

2.2.2 Topography

The bottom topography is derived from the NorKyst 800 topography. NorKyst 800 is a collaborative project between met.no, IMR and NIVA to establish an eddy resolving operational model for Norwegian coastal areas covering the coast from the Swedish border in the south to the Russian border in the north (*Albretsen et al.*, 2010).

2.2.3 Atmospheric forcing

The atmospheric variables necessary to derive momentum, heat and freshwater fluxes at the surface are extracted from archived HIRLAM12 analyzes fields. HIRLAM is met.no's operational numerical weather prediction model. The HIRLAM12 version is the core model, and as the name indicates it has a mesh size of about 12 km. Also finer mesh model versions are available, for instance HIRLAM8 and HIRLAM4, of respectively 8 and 4 km mesh size. The atmospheric variables extracted and made available to the ROMS model are the two lateral wind components at 10 meter height, the mean sea level pressure, the temperature at 2 meter height (must be specified in °K), the specific humidity at 2 meter height, the total cloud cover (in %) and the precipitation rate (must be specified in mm per 24 hours).

The HIRLAM12 analyzes fields have a temporal resolution of 24 hours. We emphasize that this somewhat low temporal resolution may result in less energy transfer from the atmosphere

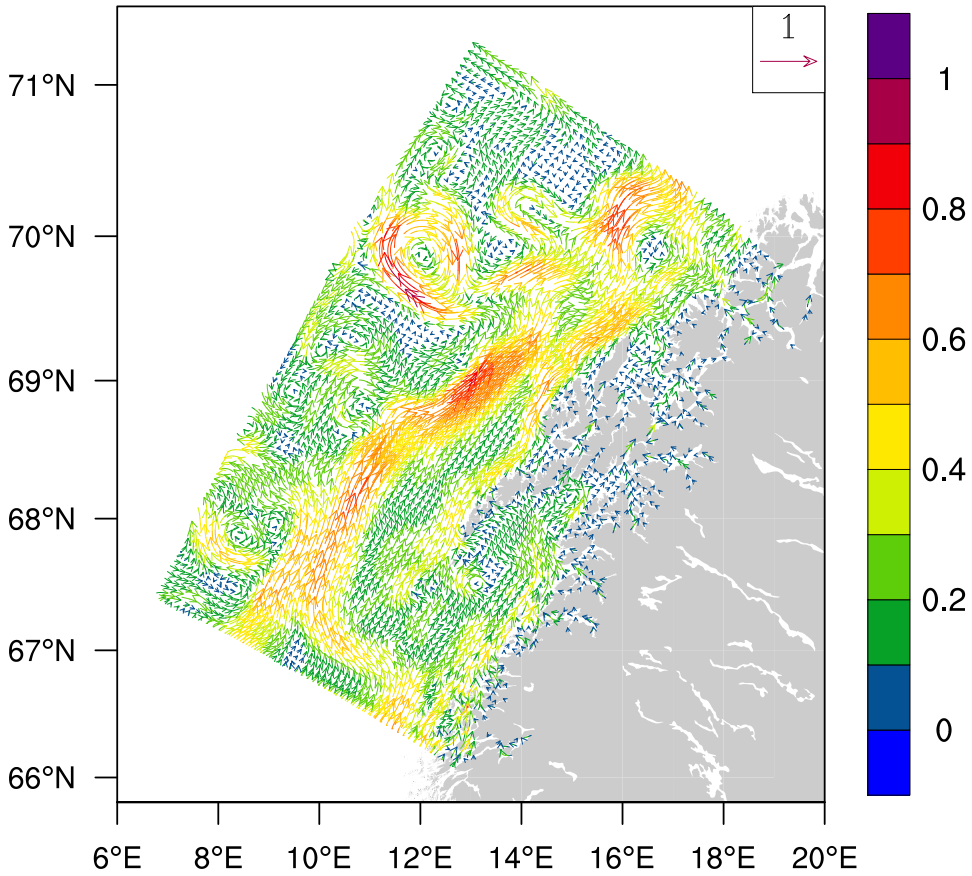

Figure 4: Displayed is the daily mean of the simulated surface currents in the Lofoten-Vesterålen area derived by the LOVECUR model August 30, 2009. The curly arrows shows the direction of the currents while their color indicate the speed in accord with the color bar to the right. Note the many jets and eddies present. Note also the dominant somewhat larger eddy located slightly north of 70°N and at about 12°E at this time.

to the ocean in comparison to applying a higher temporal resolution. Exploratory experiments using MIPOM for other coastal ocean areas (e.g., Skagerrak) and with higher temporal resolution does not show an an impact on the mesoscale activity generated (Røed 2010, personal communication). To analyze this in detail for the LV area we need to redo the simulation with a higher temporal resolution and possibly higher spatial resolution.

2.2.4 Lateral boundary forcing

The lateral boundary forcing is provided by archived analyzes fields consisting of daily mean currents, water level, temperature and salinity. The input data are extracted from the archived operational MIPOM analyzes. The archive is build up of daily mean fields saved automatically once per day based on the operational MIPOM in which the Nordic 4 km version of MIPOM is used. As indicated this version has mesh size of 4 km. It covers the entire Nordic Seas, and has open boundaries to the south and north.

At the open boundaries of MIPOM we specify monthly means of the above mentioned variables. These data are extracted from the so called EKASC archive. The latter are generated by using MIPOM with fixed hydrography to produce consistent velocity fields from a given climatology (in this case the Levitus climatology augmented with observations from the Nordic Seas region *Engedahl et al.*, 1997, 1998). The fields represent monthly means, and so lacks somewhat in temporal resolution. However they offer a fully consistent barotropic flow component, which is important for the inflows to the Nordic Seas and its throughflow.

3 Characteristics of the models

The LOVECUR model is the met.no/IMR version of the public domain model ROMS. The canonical version of the latter is described in some detail in *Haidvogel et al.* (2008). The model MIPOM that provides the lateral boundary forcing on the southern, western and northern open boundaries, is described in some detail in *Engedahl* (1995b); *Blumberg and Mellor* (1987). Here we focus on what is new and on the characteristics of the LOVECUR set up.

The version of ROMS we use is the canonical version 3.2 with extensions from IMR. The main reason for the change is to take advantage of the reworking of the ROMS at IMR with regard to tidal formulation, including the nodal correction, and the coupling to a sea-ice model. The former fixes the phase error of the previous version prominent in earlier operational products (e.g., *Røed*, 2006). The mesh sizes and number of vertical levels are given in Table 1. The ROMS simulation was completed on the supercomputer Titan. In fact it was run by people at the Norwegian Meteorological Institute with help from people at IMR.

3.1 Vertical coordinate

We note that ROMS utilizes a generalized terrain-following vertical coordinate. Terrain-following implies that the vertical levels follow the bottom contours and transform the depth coordinate from a depth coordinate to a non-dimensional vertical coordinate, in ROMS denoted s, which has the range $s \in [-1, 0]$ with $s = 0$ at the surface and $s = -1$ at the bottom. For a detailed description of vertical coordinate system in ROMS we refer to *Song and Haidvogel* (1994). For a general description we refer to *Griffies* (2004, Chapter 6). The advantage of the generalization is that it allows us to simultaneously maintaining high resolution in the surface layer in deep water as well as dealing with steep and/or tall topography. This is crucial in our case because of the steep slopes encountered in the LV area (e.g., Figure 1). Depth of the s levels can be calculated using the s-coordinate formula of *Song and Haidvogel* (1994). In the LOVECUR application we use $\theta_s = 8$, $\theta_b = 0.1$ and $hc = 10$. At a depth of -1000 meters these values gives levels at (from bottom and up) -904, -741, -611, -508, -426, -361, -308, -266, -233, -205, -183, -164, -147, -132, -117, -102, -86, -71, -56, -43, -32, -24, -18, -13, -10, -8, -6, -5, -4, -3, -2, -1.5, -1.1, -0.7, -0.2 meters, respectively for the density levels.

Table 1: Model facts

Text	Unit	ROMS
Maximum mesh size	*m*	835
Minimum mesh size	*m*	818
No. of vertical levels/layers	-	35
Horizontal dissipation	-	No explicit diffusion[1]
Vertical mixing	-	GLS mixing scheme[2]
Mode splitting	-	yes
Horizontal advection scheme	-	3rd order upwind
Long (internal) time step	*s*	45
Ratio of internal to external time step	-	15

[1]There is some weak horizontal diffusion due to the application of the third order upwind advection scheme,
[2]*Umlauf and Burchard* (2003)

3.2 Advection scheme

ROMS has a wide variety of advection schemes of relative high order. Here we use a 3rd order upwind biased scheme for the horizontal advection of momentum, salinity and temperature (*Shchepetkin and McWilliams*, 1998). In our experience this scheme has good properties in maintaining fronts and permitting mesoscale eddies and filaments. In the vertical the parabolic spline-based representation of *Shchepetkin and McWilliams* (2005) and *Haidvogel et al.* (2008) is used. This scheme gives effectively a very high order vertical advection. ROMS also offers several vertical mixing schemes. The one used here is the two-equation $k-\omega$ scheme of the Generic Length Scale (GLS) formulation of *Umlauf and Burchard* (2003). The implementation of this scheme in ROMS is documented in *Warner et al.* (2005). Note that no explicit horizontal diffusion is used. As displayed in Table 1 we emphasize that although no explicit horizontal diffusion is employed in ROMS, the 3rd order upwind scheme provides some implicit diffusion. The vertical diffusion is embedded in the GLS scheme.

3.3 Lateral forcing and open boundary conditions

The computational domain has large open boundaries to the south, west and north, at which lateral open boundary conditions are imposed. The conditions consists of daily means of the two lateral components of current, temperature, salinity and sea surface elevation. This information is extracted from the daily mean archived MIPOM analyzes once per day. The

information we extract is available at 0, 5, 10, 20, 30, 50, 100, 200, 500, and 1000 m depth. Tidal elevation and tidal currents are specified separately (Section 3.5.

A variety of open boundary conditions are available in ROMS. Here we use the recommended Chapman/Flather combination for the free surface and the 2D volume fluxes, (external mode) and for the 3D (internal mode) we use a radiation condition and nudging as described in *Marchesiello et al.* (2001) and *Albretsen et al.* (2010). The primary change we have done is to extend the nudging zone from 15 to 30 grid points. For river locations and discharges we use the same as for NorKyst800 (*Albretsen et al.*, 2010) as displayed in Figure 5. Thus the river outlets are located as close as possible to their real position in the model grid, which sometimes are at the bottom of some of the fjords that cut inland from the main shoreline. We specify the rivers as a volume flux across the land-sea boundary approximately. A vertical profile is used, giving highest flow in the upper *s*-levels.

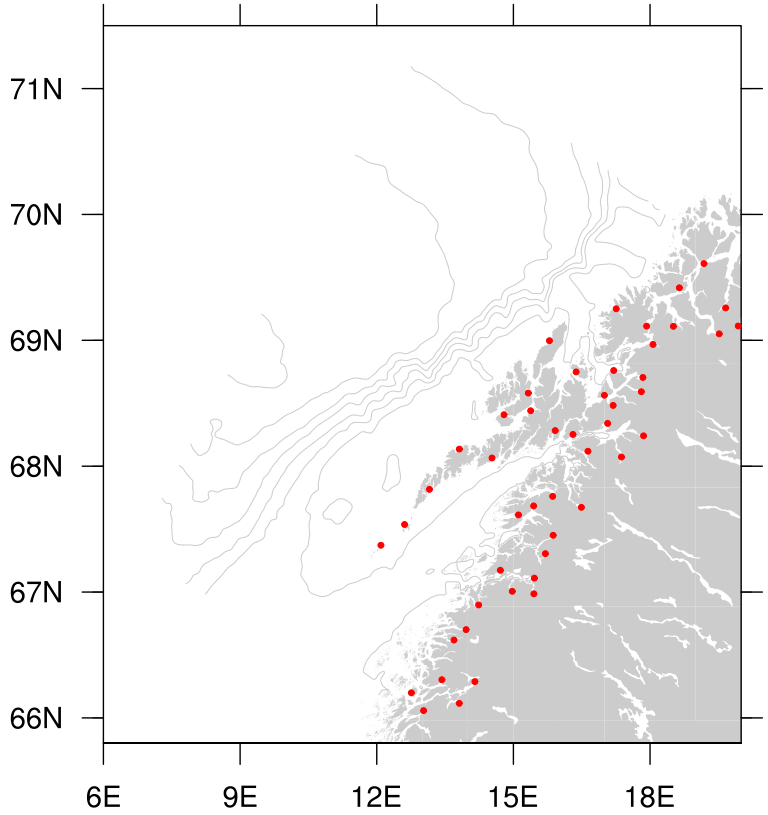

Figure 5: Displayed is is the LOVECUR model domain and topography showing the location of the river effluents (red dots). Note that the river mouths are located approximately where they discharge into the ocean, and that many of these locations are well inside the fjords.

3.4 Atmospheric forcing and bottom friction

To convert atmospheric values to a momentum and heat flux input to the model we use have replaced the standard ROMS bulk flux routine by the routines outlined in *Røed and Debernard* (2004) as described in *Albretsen et al.* (2010). The bottom friction is quadratic and follows the formulation of *Gerritsen and Bijlsma* (1988), that is,

$$\tau_b = C|\mathbf{u}_b|^2\mathbf{u}_b \tag{1}$$

where τ_b is the bottom stress, $\mathbf{u}$ is the bottom velocity and C is a constant dependent on the equilibrium depth (decreases with increasing equilibrium depth). The coefficient we use is $3.0 \cdot 10^{-3}$.

3.5 Tidal forcing

The tidal forcing of ROMS has been re-implemented at IMR, including tidal potential (not used in LOVECUR) and nodal correction. Both tidal elevation and depth integrated current is included in the boundary forcing by the aforementioned Chapman/Flather boundary condition which is designed for this purpose. Tidal information is extracted from the TPXO tidal data base. We extract eight constituents as outlined in *Albretsen et al.* (2010), namely the M_2, K_1, K_2, N_2, S_2, P_1, O_1, and Q_1 constituents.

3.6 Time stepping

To speed up the integration we use the mode splitting technique that comes with ROMS to separate the external and internal modes. It is a fairly advanced and recently developed scheme in particular regarding the exchange of information between the modes (*Shchepetkin and McWilliams*, 2005; *Haidvogel et al.*, 2008). The actual time step we use is 45 seconds for the external mode, and a ratio of 15 between external and the longer internal time step (Table 1).

4 Analysis

Hereafter we will analyse the model results. In particular we will compare the model results to temperature and salinity observations. We focus on *statistical* comparisons. As demonstrated for instance by *LaCasce and Engedahl* (2005) and *Albretsen and Røed* (2010), predictability (forecast skill) off the Norwegian coast is relatively low due to the energetic, small scale (order 10 km) eddies there. In fact we expect the eddies to be even more energetic in the present application since we employ a mesh size about five times smaller than used by *LaCasce and Engedahl* (2005) (4 km mesh size) and about two times smaller than *Albretsen and Røed* (2010) (1.5 km mesh size). Accurate predictions will therefore require widespread data assimilation, but comparing the model with such assimilation would obscure the workings of the model itself. As the latter is the focus here, a statistical comparison is the most sensible

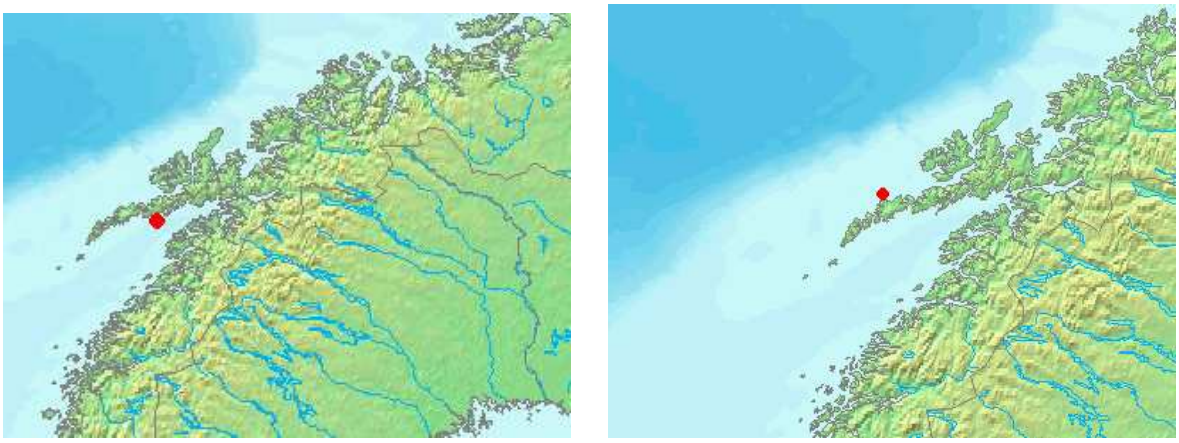

Figure 6: Displayed is the approximate postions of the IMR station Skrova (left panel) and IMR station Eggum (right panel) at which semi-continuous time series for the hindcast period exists and are extracted (in our notation denoted Station 10 and 11, respectively).

approach. Despite this fact we include scatter diagrams that includes all the IMR observations displayed in Figure 2 (blue dots).

The temperature and salinity observations available to us are extracted from the IMR hydrographic data base. We have only extracted observations that have a location inside of the LOVECUR computational domain (Figure 2). Since the IMR data did not contain any velocity measurements for this period we have no observations to compare with regarding currents and water level for the hindcast period.

For velocity observations, we use an estimate of the mean regional surface velocities, derived from the "Rio05" product of the CLS Space Oceanography Division of AVISO. Rio05 estimates the mean dynamic sea surface height for the 1993-1999 period using a multi-variate analysis of hydrographic data, surface drifter velocities and altimetry (the geoid is corrected using both the CLS01 MSS - EIGEN-GRACE 03S geoid and the NOAA (Levitus) WOA98 climatology[1], referenced to 1500 dbar). The geostrophic velocities are then estimated by differencing the sea surface height. We emphasize that the Rio05 fields are based solely on in situ and satellite data, i.e., they do not involve a numerical model. The primary drawback is that the Rio05 fields are calculated on a 50 km grid and thus capture only a smoothed version of the surface flow.

4.1 Currents

We consider first the yearly, monthly as well as daily means fields of currents and water level. The one year average spans the complete hindcast period (July 1, 2009 through June 30, 2010). We focus primarily on the means at 10 m depth, but we also show some corresponding fields at the surface.

[1] http://www.cdc.noaa.gov/cdc/data.nodc.woa98.html

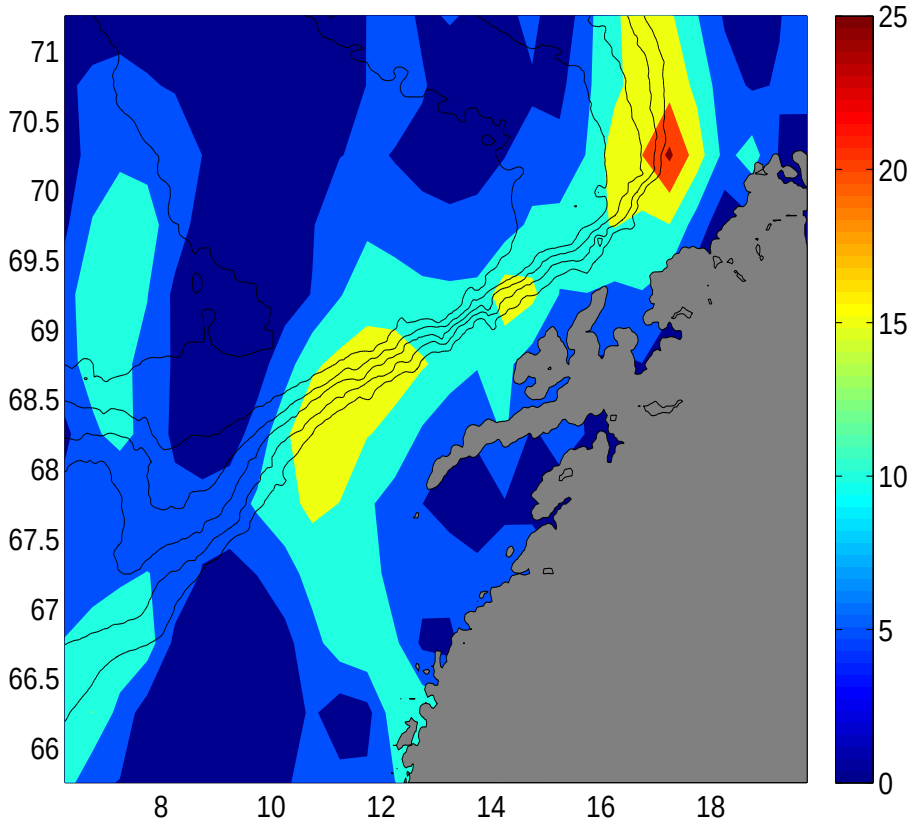

Figure 7: Surface velocities (upper panel) and speeds (lower panel) from the Rio05 product. The velocities correspond to means from the period 1993-1999. The color scale shows speed in cm/sec.

4.1.1 Observations

Contours of the horizontal velocity speeds based on the "Rio" data are shown in Figure 7. The fields are in line with circulation schemes derived from hydrography (e.g., *Mauritzen*, 1996; *Sætre*, 2007a; *Skardhamar and Svendsen*, 2005). Of primary relevance here is the inflow from the southwest consisting of an "outer branch" that follows the main shelf slope across the Vøringsplateau and an "inner branch", consisting of Norwegian Coastal Water (NCW), hugging the coast.

The "inner branch" veers offshore shortly after it enters the LOVECUR area. Only a very small fraction continues along the coast and enters the Vestfjorden. The offshore veering is caused by the constriction imposed by the Lofoten Island chain and its associated shallower shelf. The major portion that peels offshore meets the outer branch at the shelf break where it turns to the right to follow the shelf slope northward. Where the two branches meets the front intensifies. In evidence of this, and as displayed in Figure 7, the shelf slope jet associated with the front intensifies with speeds of 15-25 cm/sec as it continues northward along the shelf break. The jet reaches its maximum speed of about 25 cm/sec at about 70°N and 17°E. The maximum speeds are somewhat low compared to in situ estimates from current meters, which indicate mean speeds of up to 60 cm/sec in the upper layers of the jet. The lower speeds here

undoubtedly stem from the low resolution of the height fields.

The mean flow here is important for regional variability. The jet is known to be unstable and hence generate eddies. These eddies spread laterally away from the current cores. In addition, drifter and current meter observations (*Orvik and Niller*, 2002; *LaCasce*, 2005) suggest that due to the highly time dependent nature of the flow it is difficult to observe the flow with stationary measurements, like current meters.

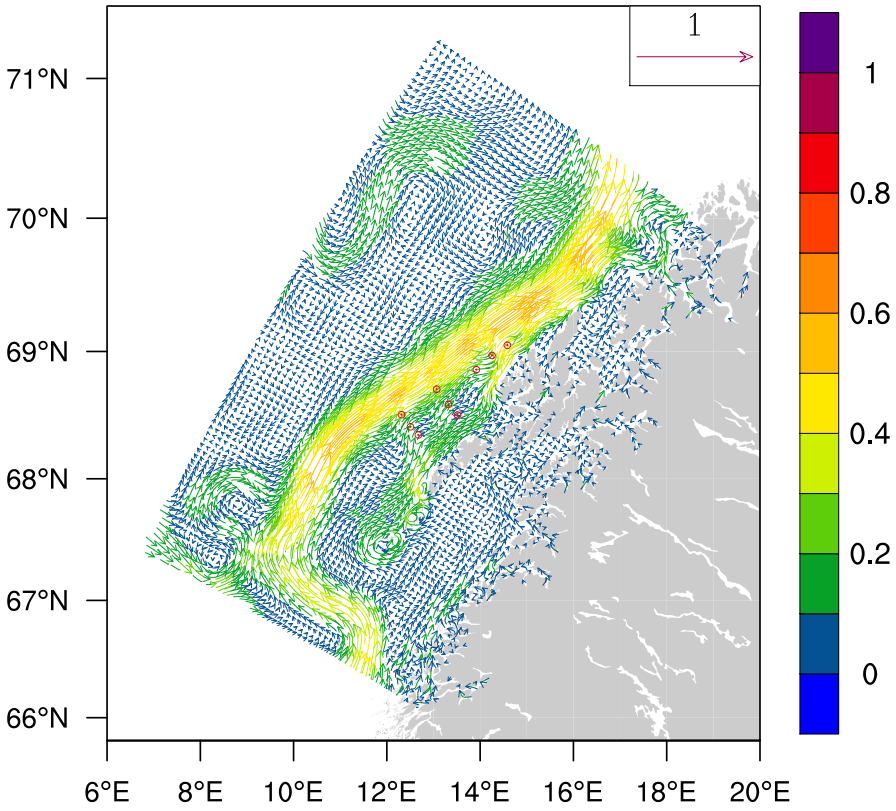

Figure 8: Displayed is the mean sea surface currents for the hindcast period (one year mean). Currents are depicted as curly vectors where its color indicates the speed in m/s in accord with the color bar to the right. The red circles indicate the position of the nine stations at which model results are extracted for analysis by a third party. We observe that all of them are situated up on the shelf where the currents are generally weaker with speeds less than 0.3 m/s. Only those closer to the shelf break are in the vicinity of the jet and thus may experience higher current speed from time to time.

4.1.2 Model results

As an example of the typical model response at 10 m, consider the yearly mean velocity vectors from the LOVECUR simulation shown in Figure 8. In line with the mean “Rio” circulation pattern shown in Figure 7 the inflow in the southwest has two branches, one hugging the coast

and one offshore follwing the shelf slope. As in the “Rio” data the inner branch meets the outer branch at the shelf breaks at which points in veers northward to flow along the shelf break west of Lofoten archipelago. Here the simulated jet intensifies which is very much in line with the “Rio” data. This circulation pattern is also in line with that of *Sætre and Aure* (2007). A primary difference between the the ROMS means and the Rio data is the strenght of the current jet. The ROMS means are generally faster (about 0.6 m/s) and is more or less uniform in speed all along the western flank of Lofoten. The “Rio” data on the other hand has a pronounced maximum at the northern end of the LOVECUR computational domain. We also note that the width of the ROMS jet is narrower than the one estimated in the Rio data. This comes at no surprise and is undoubtly due the course resolution in the Rio data as alluded to in the preceeding section.

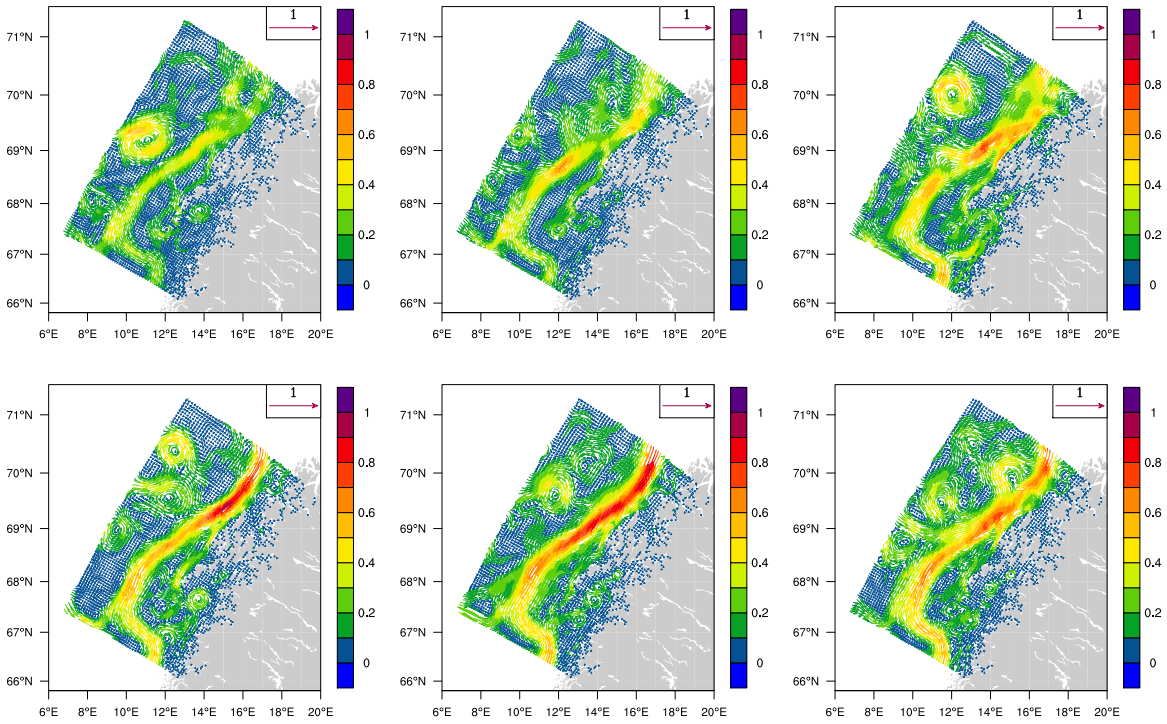

Figure 9: Monthly mean currents at 10 m depth. The upper panels shows (from left to right) July, August and September of 2009, while the lower panels show October, November and December of 2009. The figure is continued in Figure 10 showing the remaining six months of the hindcast period. Note the presence of the many robust mesoscale features showing up even in these monthly averages. In particular note the strong eddies in July and September of 2009.

According to *Sætre and Aure* (2007) a pronounced characteristic of the circulation pattern in the LV area is its high temporal and spatial variability. The models appears to capture this as illustrated by Figures 9 and 10. These figures show the twelve monthly mean currents for each month in the hindcast period. In most of them we notice the presence of a dominant eddy

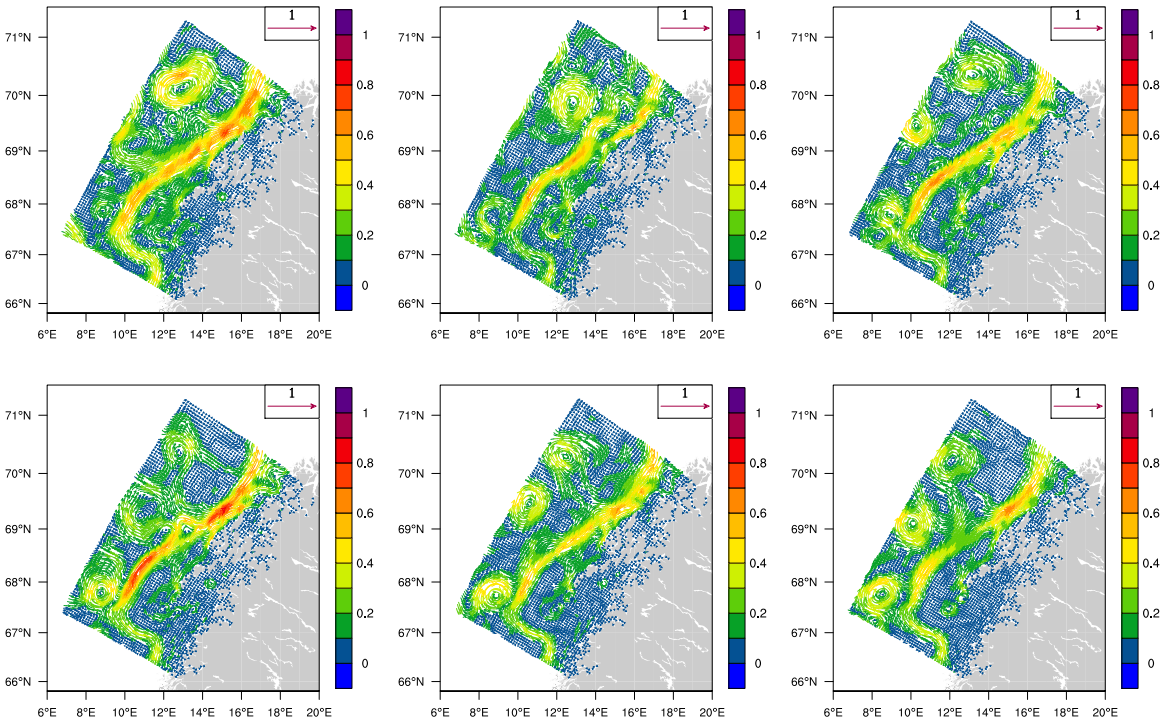

Figure 10: As Figure 9, but showing the monthly mean currents at 10 m depths for January, February and March (upper panels from left to right) and April, May and June (lower panels) of 2010.

of diameter about $\sim$ 40 - 50 km. Its location varies, but it appears to be located offshore of the shelf and the shelf slope jet, and within an area limited by 69-70°N and 10-14°E. The eddy is most pronounced in September 2009, but traces of it is visible in all monthly mean pictures. This indicates that the dominant eddy is a semi-permanent feature of lifetime at least a month or longer. We also note with interest the appearence of a series of smaller scale eddies inside the Vestfjorden in October-December of 2009. These eddies are also reported in *Sætre and Aure* (2007) to be semi-permanent features.

The reason for the richness in mesoscale features is no doubt due to the instability of the intensified front. The formation of one of them is depicted in Figure 11 showing a series of 12 daily mean surface currents two days apart starting on May 3, 2010. We note the presence of an “old” eddy generated earlier.

4.1.3 Vertical variation

Next we examine how the velocities vary in the vertical. To this end we examine the PDFs from four of the nine stations, specifically Stations 1, 7, 8 and 9. We note that these stations are the ones closest to the shelf break, while the remaining stations are further up on the shelf (Figure 12). We would therefore expect, given the high temporal variability of the circulation

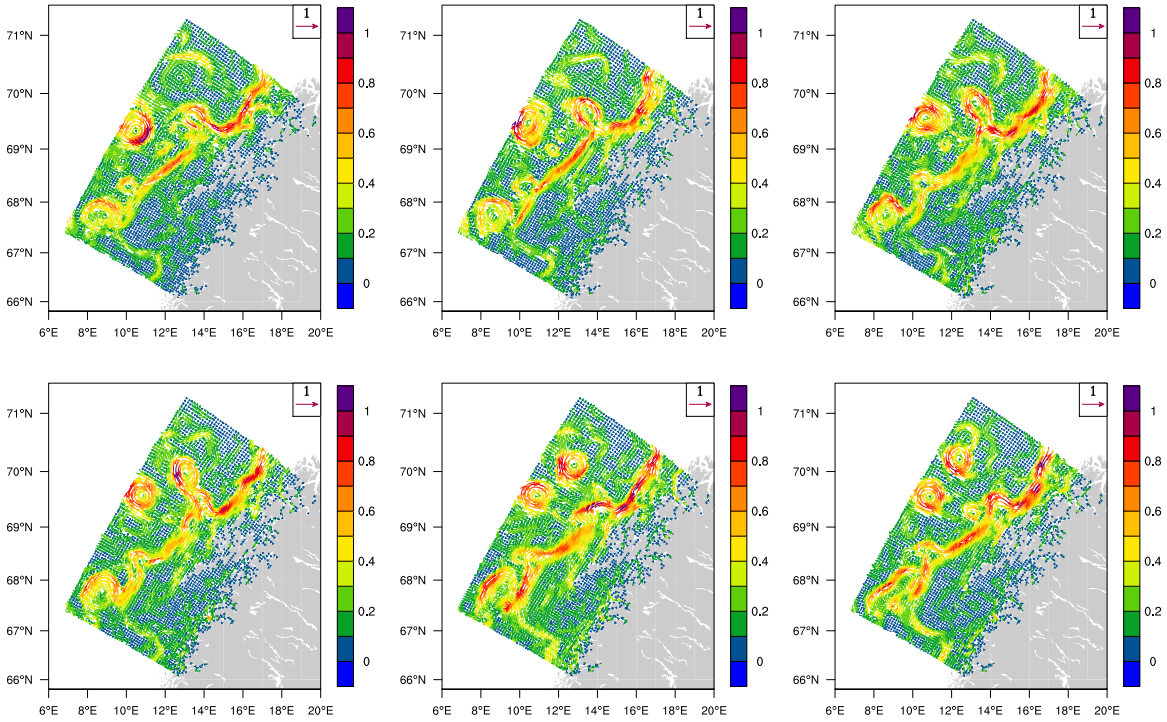

Figure 11: Eddy shedding in the model. The series shows daily mean surface currents two days apart for a twelve day period. Upper left is on May 3, 2010, while lower right is at May 8, 2010. The colors of the curly vectors indicate the current strength in accord with the color bar to the right of the figure.

pattern as shown in, e.g., Figure 11, that the shelf slope current from time to time may hit one or several of the four stations closest to the shelf break. Furthermore we note that Stations 7 and 9 are the two shallowest stations (96 and 76 m, respectively) and located on the top of hilly structures or promonteries, as is Station 7 (141 m deep), while Station 8 is the deepest (218 m) and the only one of the nine stations located in one of the many small canyons cutting into the shelf slope. We would therefore expect most pronounced directional variance with depth at the two shallow stations.

From their PDFs (Figures 13 and 14) we note that Station 9 stands out. While Stations 1, 7 and 8 all have mean speeds of about 0.15-0.25 m/s Station 9 has a mean speed of about 0.4-0.5 m/s. Moreover Station 9 has more high speed events, in particular in the upper layers (above 50 meters) where high speed events with speeds above 1 m/s occur. We also note the marked reduction in mean speed with depth below 30 m at Station 9, which is markedly less pronounced in the three other stations. This is undoubtly due to Station 9 being the shallowest station with a bottom depth of 76.3 m. The higher mean speed at Station 9 is in line with the mean field pattern shown in Figure 8. Moreover, the occurence of more frequent high speed events at this station is expected when examining the the monthly mean fields (Figures 9 and

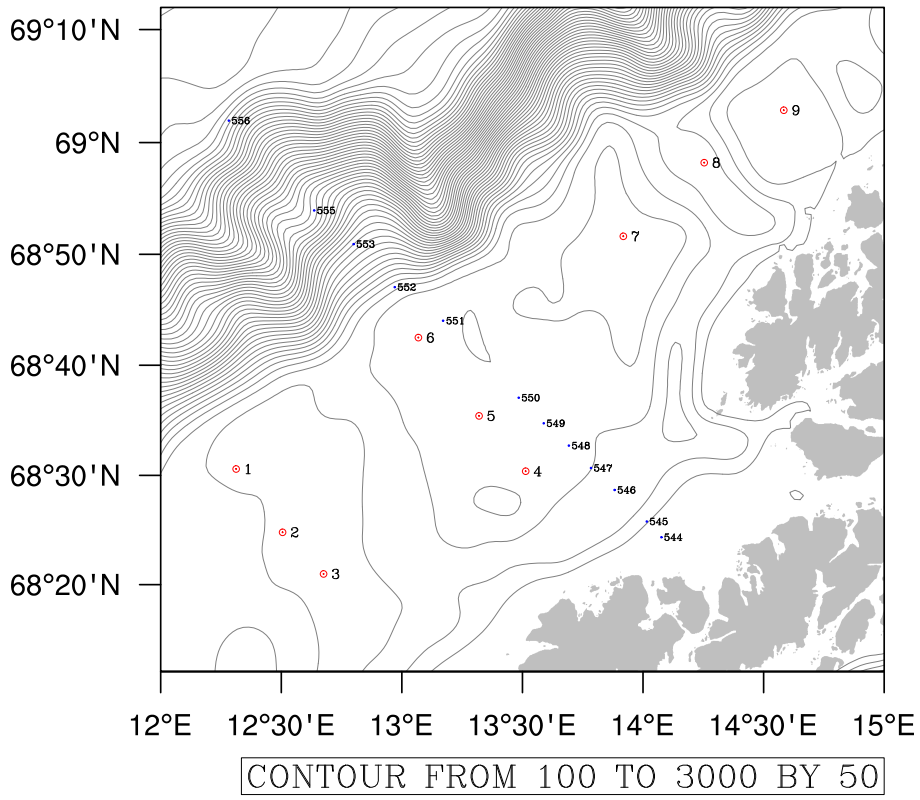

Figure 12: Location of the nine stations were data is extracted and delivered (red dots). Also shown are the stations along IMR's Gimsøy section (blue dots). Note that Station 8 is the only station located in one of the canyons cutting into the shelf. The remaining stations are located at hilly areas. We also note that Stations 1, 7, 8 and 9 are those closest to the shelf break.

10) and the daily means Figure 11, where Station 9 is clearly is closer to the slope current than any of the remaining eight stations.

Station 9 also differs drom the others with respect to the directional PDF. While Station 9 is almost unidirectional at all depths, the other three stations all have tails differing from zero at all depths indicating a somewhat higher directional spread. The most surprising is the results at Station 8. Here we expected the currents to be aligned with the direction of the canyon. However, the canyon is probably too narrow compared to the dominant length scale for such an alignment to show up in the upper layers (recall that Station 8 is 214 m deep).

4.2 Sea surface height

Next we examine the sea surface height (SSH). It should be emphasized that the SSH is the total water level changes and includes the combined effect of tides and storm surges. To extract the tidal signal we have used Pawlowicz's MATLAB toolbox T_TIDE (*Pawlowicz et al.*, 2002).

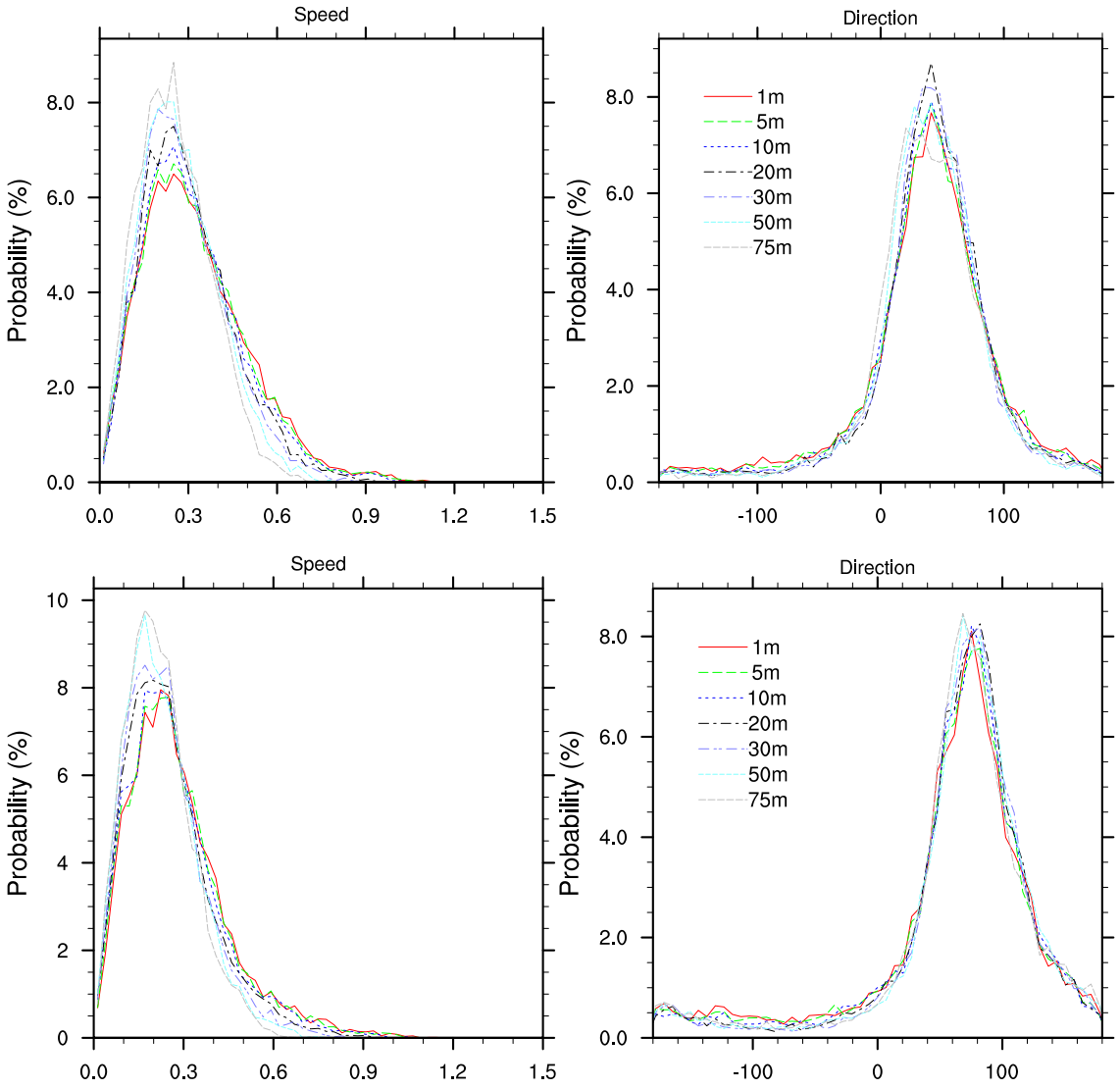

Figure 13: Frequency diagram (PDF) of the speed (m/s) and direction at various depths at Station Nos. 1 (upper panels) and 7 (lower panels). The depths are at 1, 5, 10, 20, 30, 50, and 75 meters. The model bottom depth at the stations are 141 and 96 meters, respectively. The direction is with respect to north, that is, 0° is due north while -90° is due west.

The storm surge contribution is calculated by subtracting the tidal signal from the total SSH. An example from Station 8 is displayed in Figure 15.

Examining Figure 16 reveals that the mesoscale activity is also pronounced in the SSH fields. In particular the dominant eddies shed off from the slope current are pronounced. The slope current is also visible as a marked drop in the SSH offshore.

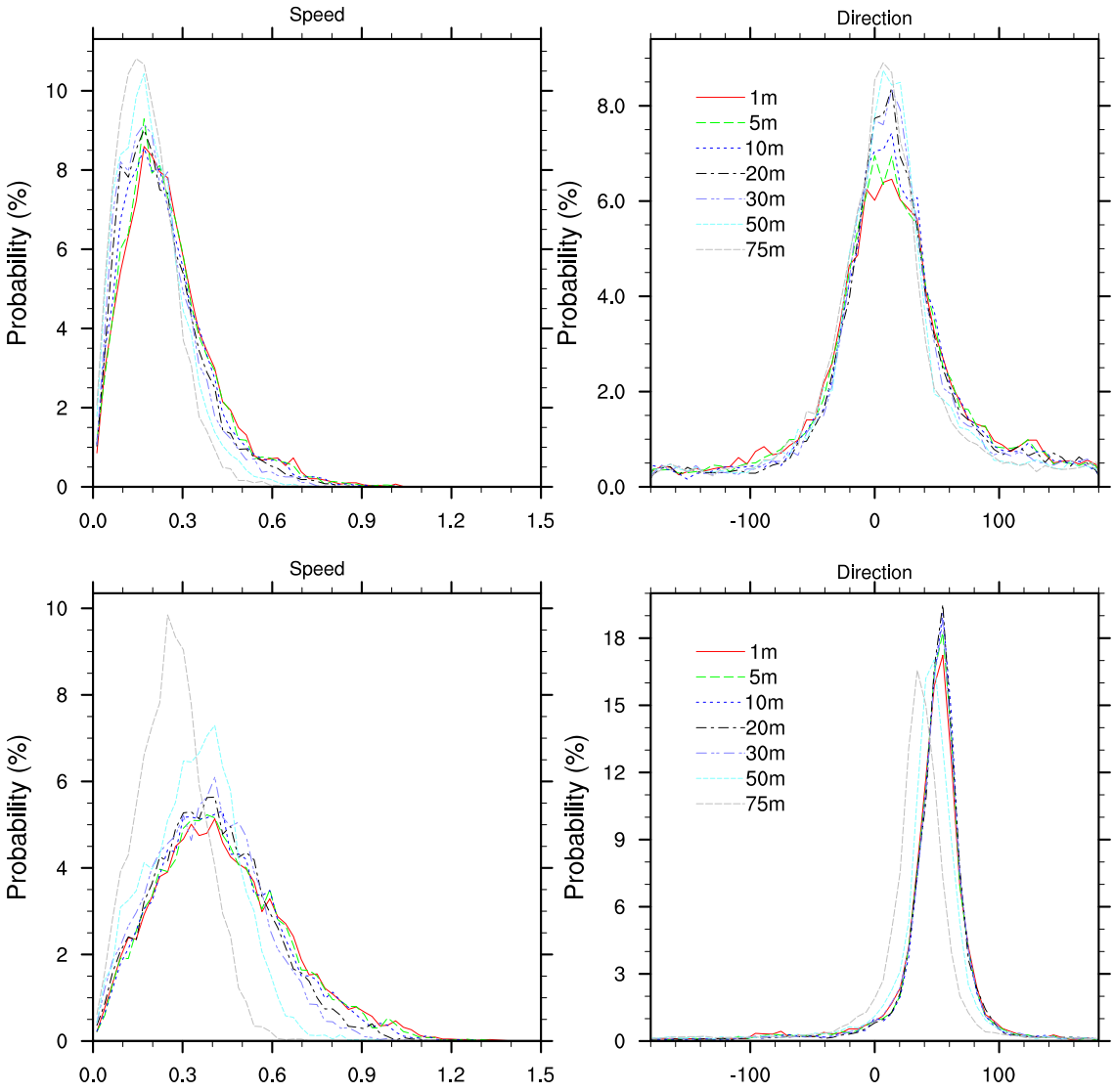

Figure 14: As Figure 13, but for Station Nos. 8 and 9. The model bottom depth at these stations are 218 and 76 meters, respectively.

4.3 Hydrography

Finally we examine the temperature and salinity. To compare model results and observations we focus on data from all of the IMR stations (the blue dots in Figure 2). Regarding time series we focus on Stations 10 and 11 (Figure 6). These are two of IMR's fixed stations along the Norwegian coast and they therefore have an almost continues data coverage while the other IMR data is more scattered in time and space.

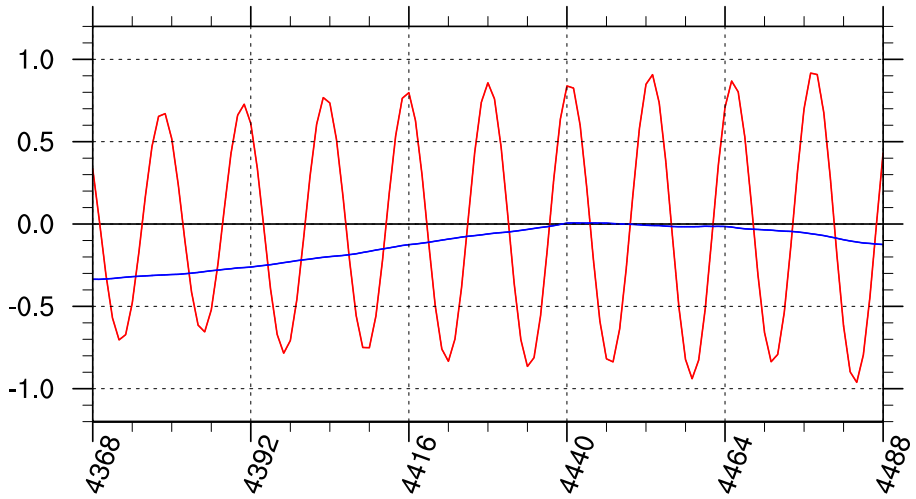

Figure 15: Depicted are the time evolutions of the predicted tidal height (red curve) and the storm surge contribution (blue curve) at Station 8. We note that the tides are the dominant signal and that the dominant variablity in the storm surge response is on the seasonal scale.

4.3.1 Model salinity fields

As shown by Figures 17 and 18, depicting the average sea surface salinity for the month of September 2009 and June 2010, respectively, the fresher NCW is transported offshore by the active eddy field. In particular we note that the core of the prominent eddy discussed in Section 4.1 (Figure 9, upper right panel) is decidedly fresher than its surrounding water.

Also to be observed are the filaments of less saline water protruding offshore off the shelf slope perhaps most pronounced in June 2010. Interestingly these dynamics are similar to what is observed and modeled in several of the worlds most prominent upwelling areas such as off the Iberian Peninsula (*Røed and Shi*, 1999, and references therein) and off the California coast (*Brink and Cowles*, 1991; *Barth*, 1994, and references therein). The primary difference is that in the upwelling areas the lighter coastal water is caused by local upwelling. Here the lighter density water (less saline) along the Norwegian coast appears because of the many freshwater sources feeding into the NCC of which the Baltic water entering the Skagerrak is the most prominent source for the NCW (*Røed and Albretsen*, 2007).

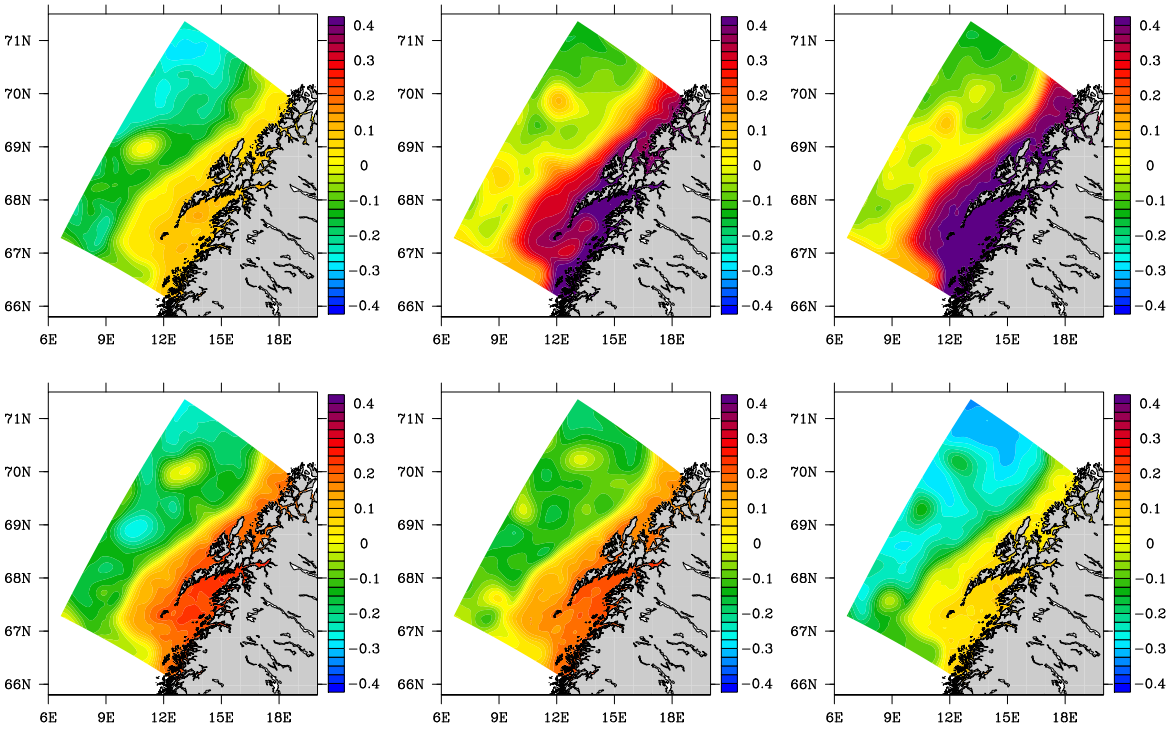

Figure 16: Monthly mean sea surface height. The upper panels shows (from left to right) July, September and November of 2009, while the lower panels show January, March and May of 2010. Note the presence of the many mesoscale features in line with Figures 9 and 10.

4.3.2 Comparison against observations

To examine the forecast skill we may examine Figure 19 showing the model against observed salinities for all IMR stations (blue dots in Figure 2) throughout the entire hindcast period at various depths. We observe that, except for the somewhat fresh bias in the four upper levels (5, 20, 50 and 100 m depth), the model is actually doing pretty well. We also observe that at 500 m both model and observation are depicting Atlantic water of 35 psu or above. At 200 m the model is clearly off the mark. This may indicate that this is in the vicinity of the pycnocline depth and thus the model may appear to have deeper mixed layer than observed.

Examining the similar scatter diagrams for temperature (Figure 20) we observe that there is a tendency for the model to underestimate the warmer temperatures above 6-7°C and to overestimate the temperatures below these values in the upper layers (above 100 m). Since the warmer temperatures happens at the end of the summer season (August-September) the model appears to be slightly too cold in the summer and too slightly to warm in the winter. In support of this we may examine the time series at Station 11 located west of the Lofoten Archipelago (Figure 6) clearly showing that the model is too cold in the summer.

The above conclusions are further supported by the PDFs for Station 11 shown in Figure 22.

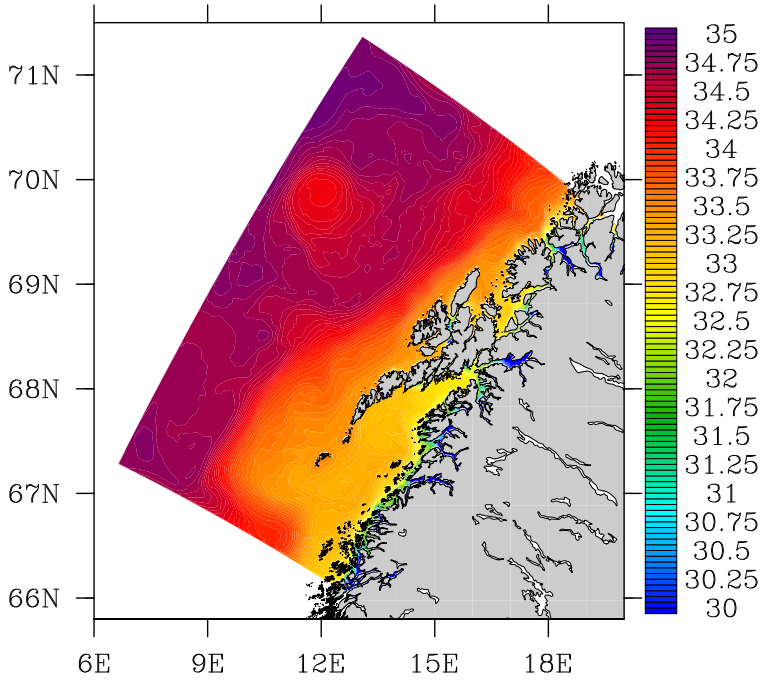

Figure 17: Average sea surface salinity for the month of September 2009. Colors indicate salinity with a contour interval of 0.25 psu as displayed by the color bar. It is interesting to note that the eddy visible in Figure 9 (upper right panel) has a fresher core than its adjacent waters. In fact the graph shows that the active eddy field is transporting the fresher NCW offshore across the shelf.

5 Summary and conclusions

We consider the results from a one year simulation employing the numerical ocean model ROMS on an eddy resolving grid (mesh size of $\sim$ 820 m) for a region along the Northern coast of Norway, specifically the Lofoten-Vesterålen (LV) area (Figure 1). ROMS employs a generalized terrain-following coordinate which allows high vertical resolution near the surface even in the deep water areas off Lofoten.

The particular aim of the study is to assess whether the simulated numerical ocean weather is able to reproduce what is observed. Ocean weather is connected to eddies, jets and meanders with a typical length scale of order 10 km in these waters. It should be emphasized that these features are responsible for most of the high current events in the ocean. The present results are to be compared with other numerical ocean weather simulations by a third party.

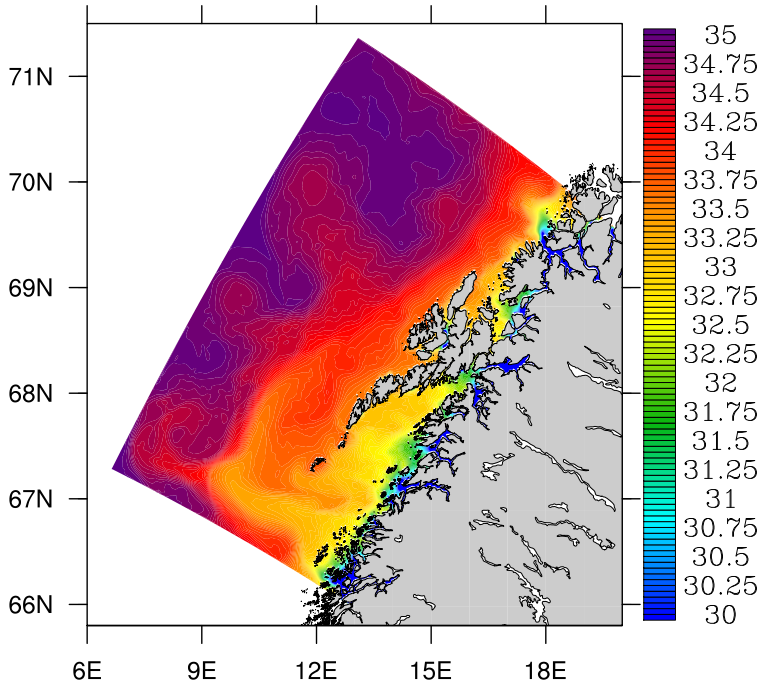

Figure 18: As Figure 18, but for the month of June 2010.

Since we at present do not have access to any current observations for the hindcast/simulation period (July 1, 2009 through June 30, 2010) we focus on a comparison with temperature and salinity data extracted from the Institute of Marine Research's hydrographic data base. In light of the active, small scale eddy field giving rise to a high spatial and temporal variability in the area (e.g., Figure 11) we focus on *statistical* comparisons of time series. In addition we have examined the spatial structure (lateral and vertical) of the velocity means (yearly, monthly and daily means) at different depths.

The simulated one year mean flow (Figure 8) is generally in line with a similar product constructed from observations alone (Figure 7). A primary difference is that the ROMS mean along-slope jet is narrower and more energetic than the jet estimated from observations, with generally higher speeds in the ROMS means. The flow pattern is however very similar with an intensification of the northward flowing jet west of Lofoten. The jet is clearly baroclinically unstable (*Shi and Røed*, 1999; *Fossum and Røed*, 2006) shedding off eddies of diameter $\sim$ 40-50 km, and a host of smaller scale eddies (Figure 11). The larger scale eddy is a long-lived feature once formed and hence shows up in the monthly mean fields as well (Figure 9).

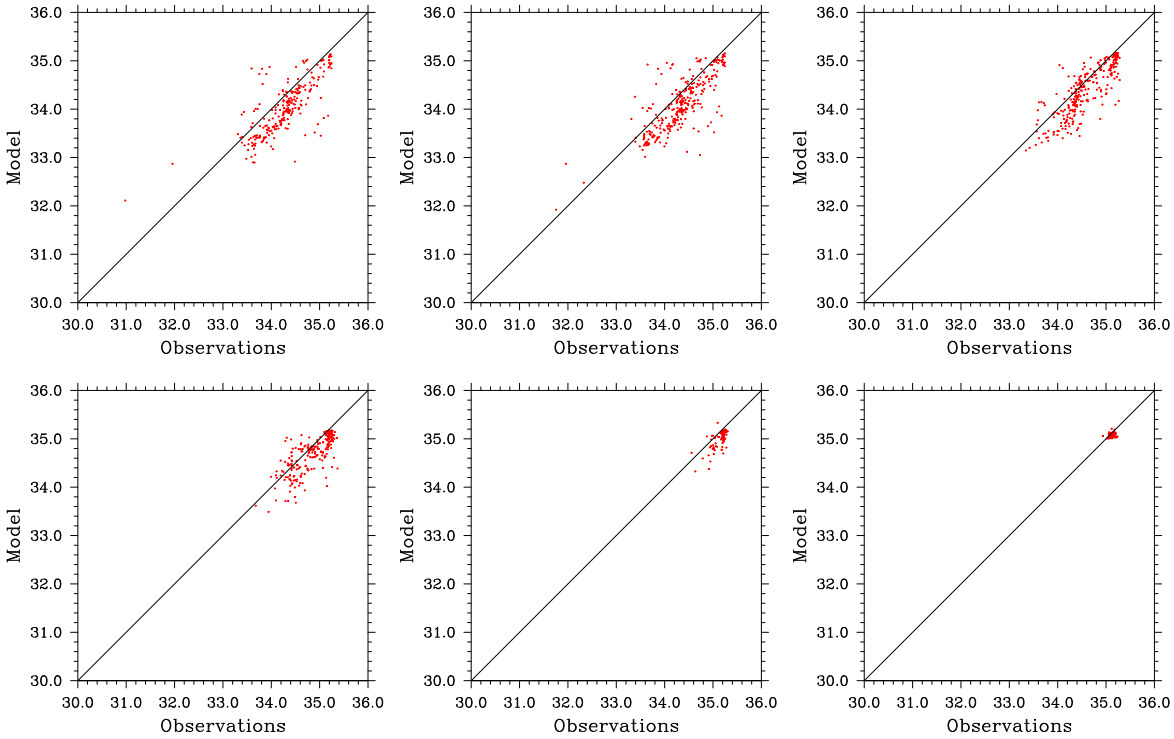

Figure 19: Scatter diagram of salinity extracted from all IMR stations (Figure 2 for 5, 10, 50, 100, 200, and 500 meters. Observations is along the horizontal axis, while model results are shown along the vertical axis. The scale is from 30 to 36 psu.

A comparison of the observed temperature and salinity with those of ROMSreveals that the model has a fresh bias of about 0.3 psu. Also revealed is that model tends to be too cold in the summer and too warm in the winter.

Acknowledgment

This research was supported in parts by a consortium of offshore industry companies through Statoil Petroleum AS, Contract No. 4502047180. The computations were performed at the Norwegian Supercomputer facilities. We thank Pål Erik Isachsen for constructing Figure 7 and Jon Albretsen for many helpful discussions on the subject. In particular we are grateful for the help offered by Jon Albretsen and Ann Kristin Sperrevik regarding setting up the NorKyst800 model for this application.

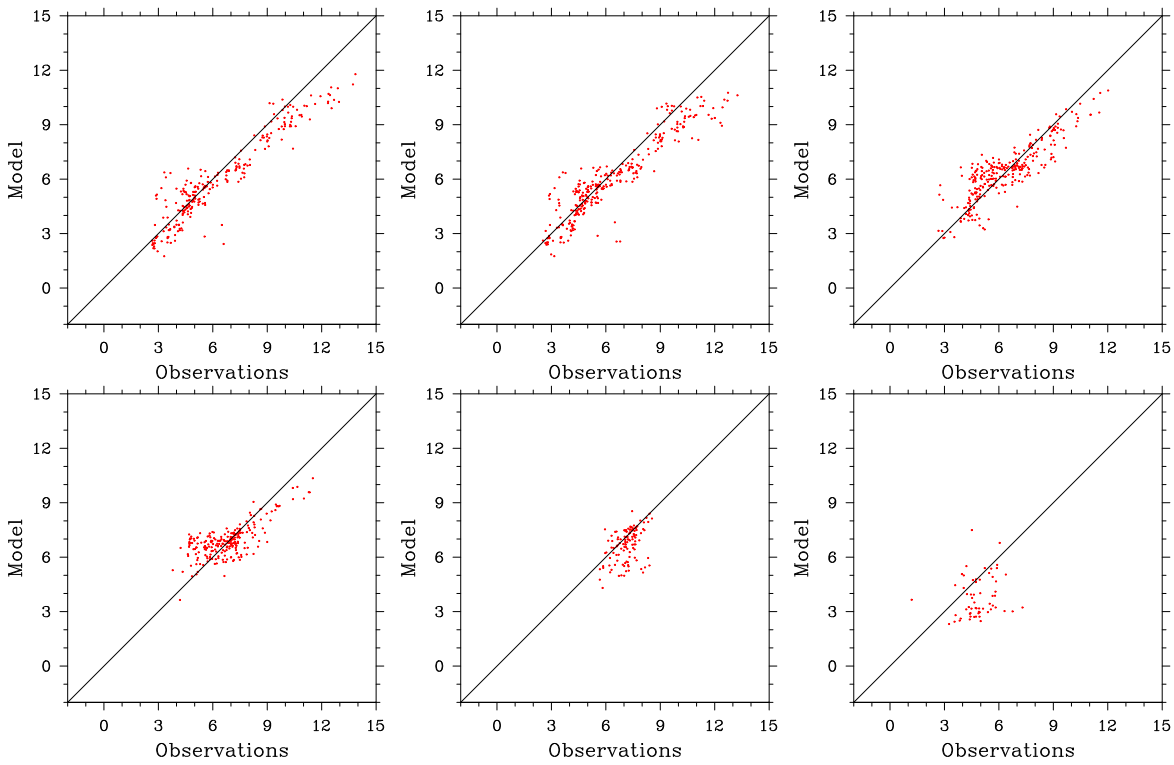

Figure 20: As Figure 19, except showing temperature rather than salinity. The scale is from -2.0°C to 15.0°C.

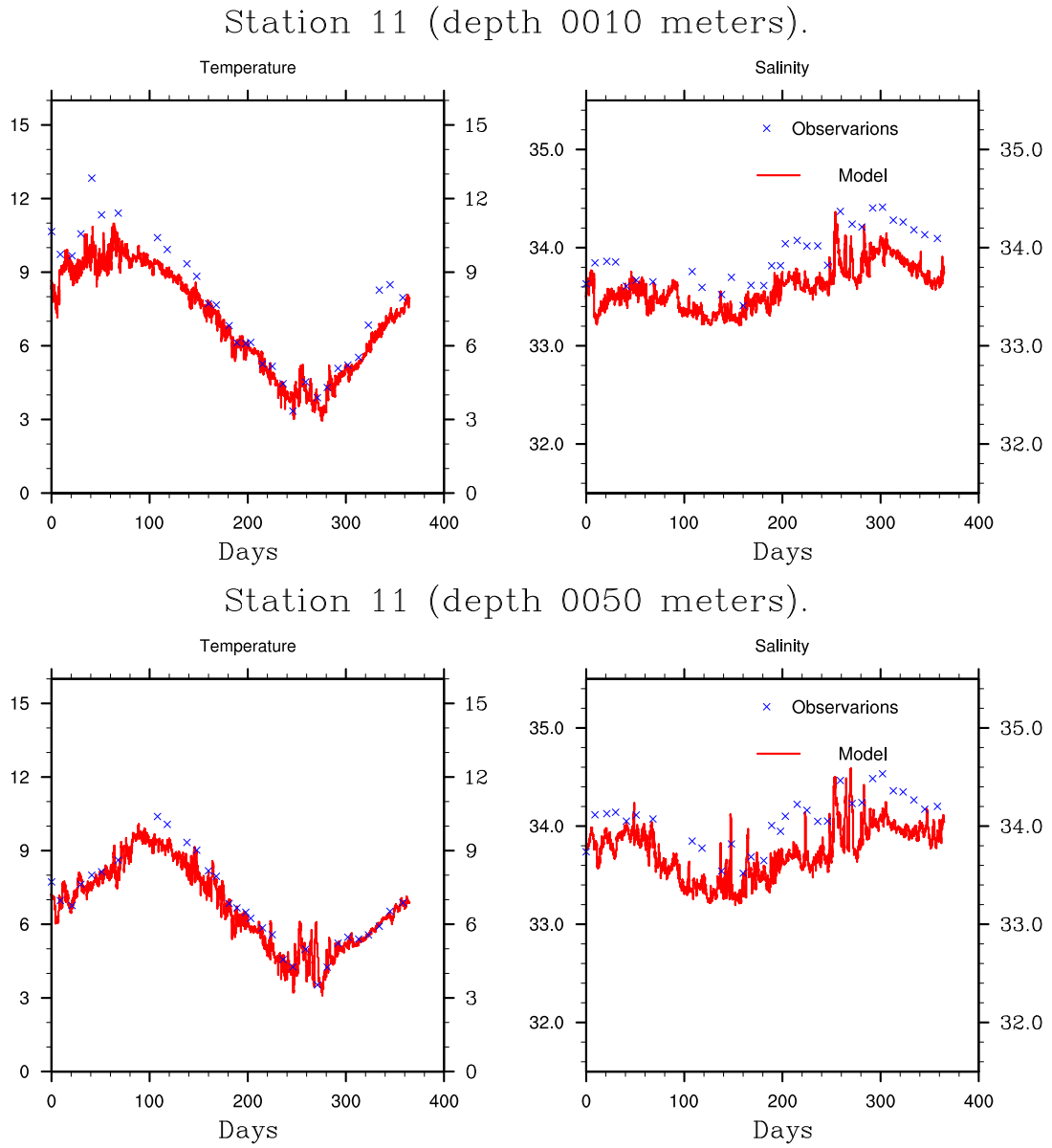

Figure 21: Time series of temperature (left panel) and salinity (right panel) for Station 11 Eggum. Red curves correspond to model results, while the observations are denoted with blue crosses.

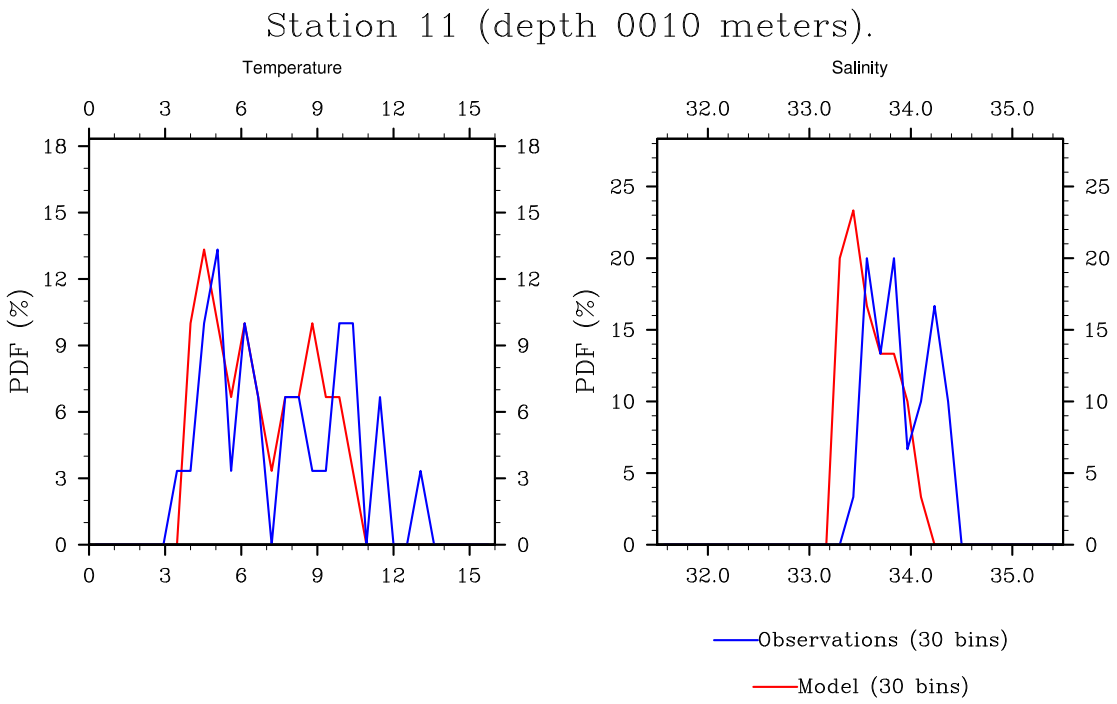

Figure 22: As Figure 13, but for Station Nos. 11.

References

Albretsen, J. (2007), The impact of freshwater discharges on the ocean circulation in the Skagerrak/northern North Sea area. part ii: energy analysis, *Ocean Dynamics*, *57*, 287–304, doi:10.1007/s10236-007-0121-6.

Albretsen, J., and L. P. Røed (2010), Decadal long simulations of mesoscale structures in the North Sea/Skagerrak using two ocean models, *Ocean Dynamics*, *60*, 5–36, doi: 10.1007/s10236-010-0296-0.

Albretsen, J., A. K. Sperrevik, A. Staalstrøm, A. D. Sandvik, F. Vikebø, and L. Asplin (2010), Norkyst-800 report no. 1: User manual and technical descriptions, *Technical memorandum*, met.no, IMR, NIVA, in preparation.

Barth, J. B. (1994), Short-wavelength instabilities on coastal jets and fronts, *J. Geophys. Res.*, *99*, 16,095–16,115.

Blumberg, A., and G. Mellor (1987), A description of a three-dimensional coastal ocean circulation model., in *Three-dimensional Coastal Ocean Models, Coastal and Estuarine Sciences*, vol. 4, edited by N. Heaps., pp. 1–16, American Geophys. Union.

Brink, K., and T. J. Cowles (1991), The coastal transition zone program, *J. Geophys. Res.*, *96*, 14,637–14,647.

Engedahl, H. (1995b), Implementation of the Princeton ocean model (POM/ECOM-3D) at the Norwegian Meteorological Institute (DNMI)., *Research Report 5*, Norwegian Meteorological Institute.

Engedahl, H., and L. P. Røed (1999), Forecasting ocean currents in deep water areas: The Ormen Lange case (1997), *Research Report 80*, Norwegian Meteorological Institute, Box 43 Blindern, N-0313 Oslo, Norway.

Engedahl, H., G. Eriksrød, C. Ulstad, and B. Ådlandsvik (1997), Climatological oceanographic archives covering the Nordic Seas and the Arctic Ocean with adjacent waters, *Research Report 59*, Norwegian Meteorological Institute, Box 43 Blindern, N-0313 Oslo, Norway.

Engedahl, H., B. Ådlandsvik, and E. A. Martinsen (1998), Production of monthly mean climatological archives for the Nordic Seas, *J. Mar. Syst.*, *14*, 1–26.

Engedahl, H., A. Lunde, A. Melsom, and X. B. Shi (2001), New schemes for vertical mixing in MI-POM and MICOM, *Research Report 118*, Norwegian Meteorological Institute, ISSN 0332-9879.

Fossum, I. (2006), Analysis of instabilities and mesoscale motion off southern Norway, *J. Geophys. Res.*, *111, C08006*, doi:10.1029/2005JC003228.

Fossum, I., and L. P. Røed (2006), Analysis of instabilities and mesoscale motion in continuously stratified ocean models, *J. Mar. Res.*, *64*, 319–353.

Gerritsen, H., and A. C. Bijlsma (1988), *Computer Modelling in Ocean Engineering*, chap. Modelling of tidal and wind driven flow: The Dutch Continental Shelf Model, p. 9 pp., Schrefler & Zienckiewicz, Rotterdam, Balkema.

Griffies, S. M. (2004), *Fundamentals of ocean climate models*, Princeton University Press.

Hackett, B., and H. Engedahl (2000), Numerical model study of slope and Deep Water Currents. PhaseIII: Regional archive evaluation and Ormen Lange hindcast, *Research Report 93*, Norwegian Meteorological Institute, Box 43 Blindern, N-0313 Oslo, Norway.

Haidvogel, D. B., H. Arango, P. W. Budgell, B. D. Cornuelle, E. Curchitser, E. D. Lorenzo, K. Fennel, W. R. Geyer, A. J. Hermann, L. Lanerolle, J. Levin, J. C. McWilliams, A. J. Miller, A. M. Moore, T. M. Powell, A. F. Shchepetkin, C. R. Sherwood, R. P. Signell, J. C. Warner, and J. Wilkin (2008), Ocean forecasting in terrain-following coordinates: Formulation and skill assessment of the regional ocean modeling system, *J. Comput. Phys.*, *227*(7), 3595–3624, doi:http://dx.doi.org/10.1016/j.jcp.2007.06.016.

Jenkins, A. D., H. Engedahl, B. Hackett, and B. Å. Hjøllo (2001), Validation of water level predictions in Norwegian waters, *Research report no. 105*, Norwegian Meteorological Institute, Oslo, Norway.

LaCasce, J. H. (2005), Statistics of low frequency currents over the western Norwegian shelf and slope I: current meters, *Ocean Dyn.*, *55*, 213–221, doi 10.1007/s10,236–005–0021–6.

LaCasce, J. H., and H. Engedahl (2005), Statistics of low frequency currents over the western Norwegian shelf and slope II: Model, *Ocean Dyn.*, *55*, 222–237, doi 10.1007/s10,236–005–0022–5.

Marchesiello, P., J. C. McWilliams, and A. F. Shchepetkin (2001), Open boundary conditions for long-term integration of regional ocean models, *Ocean Mod.*, *3*, 1–20.

Martinsen, E. A., H. Engedahl, B. Hackett, H. Tønnesen, O. Høvik, and B. Ådlandsvik (1995), Metocean MOdeling Project: Hindcast simulations of the ocean response to storm events for the Haltenbanken, the Vøringsplateau and the barents sea, *Research report no. 6*, Norwegian Meteorological Institute, Oslo, Norway.

Mauritzen, C. (1996), Production of dense overflow waters feeding the north atlantic across the greenland-scotland ridge. part 1: Evidence for a revised circulation scheme, *Deep Sea Research*, *43*, 769–806.

Orvik, K. A., and P. Niller (2002), Major pathways of Atlantic water in the northern North Atlantic and Nordic Seas toward Arctic, *Geophys. Res. Lett.*, *29(19)*, 1896, doi:10102.

Pawlowicz, R., B. Beardsley, and S. Lentz (2002), Classical tidal harmonic analysis including error estimates in MATLAB using T_TIDE, *Computers and Geosciences*, *28*, 929–937.

Røed, L. P. (2006), CONMAN Technical Report no. 1: Documentation of models and experimental set-up, *met.no Report 05/2006*, Norwegian Meteorological Institute, Box 43 Blindern, N-0313 Oslo, Norway.

Røed, L. P., and J. Albretsen (2007), The impact of freshwater discharges on the ocean circulation in the Skagerrak/northern North Sea area. Part I: model validation, *Ocean Dynamics*, *57*, 269–285, dOI: 10.1007/s10236-007-0122-5.

Røed, L. P., and J. Debernard (2004), Description of an integrated flux and sea-ice model suitable for coupling to an ocean and atmosphere model, *met.no Report 4/2004*, Norwegian Meteorological Institute, P.O. Box 43 Blindern, 0313 Oslo, Norway.

Røed, L. P., and I. Fossum (2004), Mean and eddy motion in the Skagerrak/northern North Sea: insight from a numerical model, *Ocean Dynamics*, *54*, 197–220.

Røed, L. P., and X. B. Shi (1999), A numerical study of the dynamics and energetics of cool filaments, jets and eddies off the Iberian Peninsula, *J. Geophys. Res.*, *104*, 29,817–29,841.

Røed, L. P., I. Fossum, and A. Carrasco (2010), Towards eddy resolving ocean prediction off the northern coast of Norway., in *Coastal to Global Operational Oceanography: Achievements and Challenges. Proceedings of the Fifth International Conference on EuroGOOS*, vol. EuroGoos Publ. No. 28, edited by H. Dahlin, M. Bell, N. C. Flemming, and S. E. Petersson, pp. 246–252, EuroGOOS Office, SMHI, 601 76 Norrkøping, Sweden, ISBN 978-91-974828-6-8.

Sætre, R. (Ed.) (2007a), *The Norwegian Coastal Current - Oceanography and Climate*, 159 pp., Tapir Academic Press, Trondheim, Norway, ISBN 978-82-519-2184-8.

Sætre, R. (2007b), Studies of the coastal region. Background and history, in *The Norwegian Coastal Current - Oceanography and Climate*, edited by R. Sætre, pp. 19–34, Tapir Academic Press, Trondheim, Norway, ISBN 978-82-519-2184-8.

Sætre, R. (2007c), Properties of the coastal water masses, in *The Norwegian Coastal Current - Oceanography and Climate*, edited by R. Sætre, pp. 19–34, Tapir Academic Press, Trondheim, Norway, ISBN 978-82-519-2184-8.

Sætre, R., and J. Aure (2007), Characteristic circulation features, in *The Norwegian Coastal Current - Oceanography and Climate*, edited by R. Sætre, pp. 19–34, Tapir Academic Press, Trondheim, Norway, ISBN 978-82-519-2184-8.

Shchepetkin, A., and J. McWilliams (2005), The Regional Ocean Modeling System (ROMS): A split-explicit, free-surface, topography-following coordinate ocean model, *Ocean Modelling*, *9*, 347–404.

Shchepetkin, A. F., and J. McWilliams (1998), Quasi-monotone advection schemes based on explicit locally adaptive dissipation, *Mon. Wea. Rev.*, *126*, 1541–1580.

Shi, X. B., and L. P. Røed (1999), Frontal instability in a two-layer, primitive equation ocean model, *J. Phys. Oceanogr.*, *29*, 948–968.

Skardhamar, J., and H. Svendsen (2005), Circulation and shelf-ocean interaction off North Norway, *Cont. Shelf Res.*, *25*, 1541–1560.

Song, T., and D. Haidvogel (1994), A semi-implicit ocean circulation model using a generalized topography-following coordinate system, *J. Comput. Phys.*, *115*(228-244).

Umlauf, L., and H. Burchard (2003), A generic length-scale equation for geophysical turbulence models, *J. Marine Res.*, *61*, 235–265.

Warner, J. C., C. Sherwood, H. Arango, and R. Signell (2005), Performance of four turbulence closure methods implemented using a generic length scale method, *Ocean Mod.*, *8*, 81–113.